NEOPLASIA
www.neoplasia.com
Volume 23 Number 7 July 2021 pp. 692–703

Original Research

Exosomal lncRNA NEAT1 from cancer-associated fibroblasts facilitates endometrial cancer progression via miR-26a/b-5p-mediated STAT3/YKL-40 signaling pathway ☆

Jiang-Tao Fan*; Zhao-Yu Zhou; Yan-Lu Luo; Qin Luo; Si-Bang Chen; Jin-Che Zhao; Qiao-Ru Chen

Department of Obstetrics and Gynecology, The First Affiliated Hospital of Guangxi Medical University, Nanning 530021, Guangxi Province, PR China

Abstract

Cancer-associated fibroblasts cells (CAFs) confer a rapid growth and metastasis ability of endometrial cancer (EC) via exosomes-mediated cellular communication. Long non-coding RNA nuclear enriched abundant transcript 1 (lncRNA NEAT1) drives the malignant phenotypes of EC cells. However, the role of exosomal NEAT1 from CAFs in EC progression remains ambiguous, which needs to be investigated. In our study, NEAT1 and YKL-40 were up-regulated, while miR-26a/b-5p was down-regulated in EC tissues. Moreover, NEAT1 expression was increased in CAF-exosomes compared with that in NF-exosomes. In addition, the exosomal NEAT1 derived from CAFs could transfer to EC cells and promote YKL-40 expression. Further exploration showed that exosomal NEAT1 enhanced YKL-40 expression via regulating miR-26a/b-5p-STAT3 axis in EC cells. More importantly, exosomal NEAT1 accelerated *in vivo* tumor growth via miR-26a/b-5p-STAT3-YKL-40 axis. Taken together, our study reveals that exosomal NEAT1 from CAFs contributes to EC progression via miR-26a/b-5p-mediated STAT3/YKL-40 pathway, which indicates the therapeutic potential of exosomal NEAT1 for treating EC.

Neoplasia (2021) 23, 692–703

Keywords: EC, CAFs, exosome, NEAT1, miR-26a/b-5p-STAT3-YKL-40 axis

Introduction

Endometrial cancer (EC) is one of prevalent malignancies of women worldwide, causing about 12,160 deaths in 2019 [1]. An increased prevalence of EC has been found particularly in socioeconomic transforming countries [2]. In spite of surgical removal of macroscopic tumor combined reasonable chemotherapy, the EC patients may suffer from recurrent even metastatic tumors [3]. Up to now, the exact pathogenesis of EC has not been completely explained. Chitinase 3 like 1 (YKL-40/CHI3L1) protein is a member of chitinase family. The elevated expression of YKL-40 is observed in many malignant tumors, which drives tumor growth, angiogenesis and metastasis [4,5]. Previous studies suggest that YKL-40 is up-regulated in the serum and endometrial carcinoma samples of EC patients, and correlates with a poor prognosis [6,7]. Li et al. indicated that depletion of YKL-40 led to a remarkable inhibition of growth and invasion in EC HEC-1A cells [8]. These findings strongly revealed that YKL-40 was essential for the malignant development of EC. It is noteworthy that the transcription and expression of YKL-40 is regulated by signal transducers and activators of transcription 3 (STAT3) in glioma cells, which controls glioma migration [9]. Notwithstanding the crucial roles of YKL-40 in EC progression, little is known about the regulatory mechanisms upstream of YKL-40. Whether YKL-40 expression is regulated by STAT3 in EC needs to be further explored.

Abbreviations: EC, endometrial cancer; YKL-40/CHI3L1, chitinase 3 like 1; miRNAs, microRNAs; CAFs, cancer-associated fibroblasts cells; lncRNAs, long non-coding RNAs; NEAT1, nuclear enriched abundant transcript 1; STAT3, signal transducers and activators of transcription 3; NFs, normal fibroblasts; ceRNAs, competing endogenous RNA; si-Rab27a, siRNA for Rab27a; sh-Rab27a, shRNA for Rab27a; TEM, transmission electron microscopy; WT, wild type; MUT, mutant type; MS2bp, MS2-binding protein; ChIP, chromatin immunoprecipitation.

* Corresponding author.
E-mail address: fanjiangtaofjt416@163.com (J.-T. Fan).

☆ Conflicts of Interest: The authors declare that they have no conflict of interest.

Received 1 February 2021; received in revised form 20 April 2021; accepted 5 May 2021

https://doi.org/10.1016/j.neo.2021.05.004

MicroRNAs (miRNAs) have been recognized as pivotal regulators of malignant tumors through inhibiting transcription of tumor-related genes. Previous studies have indicated that both miR-26a-5p and miR-26b-5p are regarded as anti-oncogenes and down-regulated in a wide variety of tumors [10-12]. However, the dysregulation and functional role of miR-26a/b-5p in EC has been rarely investigated. Bioinformatics analysis results suggested that STAT3 might be a target of miR-26a/b-5p. Given these data, we hypothesized that miR-26a/b-5p might directly inhibit STAT3 expression, and then reduce downstream YKL-40 level in EC, thus delaying EC progression.

It is well known that cancer-associated fibroblasts cells (CAFs), one of important types of stromal cells, promote the progression of cancer via releasing cytokines, chemokines or exosomes that mediate intercellular communication [13,14]. A previous study revealed that exosomes derived from CAFs affected the metastasis of EC [15]. Long non-coding RNAs (lncRNAs) without protein-coding ability are emerging as regulators of various cancers. Interestingly, lncRNAs have been enriched in exosomes and served as communicators between CAFs and tumor cells [13]. LncRNA nuclear enriched abundant transcript 1 (NEAT1) has been shown to be up-regulated in EC, and accelerate the malignant growth and metastasis of EC cells [16,17]. In addition, NEAT1 is predicted to bind to miR-26a/b-5p by bioinformatic analysis. Despite this, whether NEAT1 might be in exosomes released from CAFs and affect EC progression via targeting miR-26a/b-5p-STAT3-YKL-40 axis remains ambiguous.

To test the above hypothesis, an *in vitro* co-culture model of CAFs and EC cells was established. We found an increased level of NEAT1 in exosomes derived from CAFs. Moreover, exosomal NEAT1 enhanced STAT3 and YKL-40 expression in EC cells via sponging miR-26a/b-5p. Finally, exosomal NEAT1 drove tumorigenesis in nude mice via regulating miR-26a/b-5p-STAT3-YKL-40 axis. Taken together, our results uncover a novel network mediated by exosomal NEAT1 during EC progression, which sheds light on a potential therapeutic strategy for EC.

Materials and methods

Clinical samples

Clinical samples were obtained from 30 EC patients from the First Affiliated Hospital of Guangxi Medical University. Normal endometrial specimens were collected from 30 patients with uterine myoma. No systemic treatment was given to patients before sampling. Written informed consent was obtained from all patients. The clinical samples were kept in liquid nitrogen before detection. Ethical approval was acquired from Ethics committee of the First Affiliated Hospital of Guangxi Medical University.

Cell culture and treatment

Human EC cell lines HEC-1A, HEC-1B, and RL95-2 were purchased from ATCC (Manassas, VA, USA). Human endometrial epithelial cell lines were obtained from Procell Life Science & Technology co., Ltd. (Wuhan, China). The cells were cultured in culture medium (McCoy's 5a for HEC-1A; EMEM for HEC-1B; DMEM/F12 for RL95-2; specific medium provided by Procell for human endometrial epithelial cell lines) containing 10% fetal bovine serum at 37 °C with 5% CO_2. According to a previous study [18], CAFs and normal fibroblasts (NFs) were separated from human EC tissues and normal endometrial tissues, respectively. The isolated CAFs and NFs were cultured in DMEM/F12 containing 10% fetal bovine serum. For identification, the primary CAFs and NFs were detected by immunofluorescence staining of CAF-specific markers (α-SMA and vimentin) as described below. To inhibit exosome secretion, CAFs were treated with 20 μM GW4869 (Selleck, Houston, TX, USA) or infected with lentivirus expressing siRNA for Rab27a (si-Rab27a). To silence or overexpress NEAT1, CAFs were infected with the lentivirus containing sh-NEAT1 or NEAT1 gene. Lentivirus containing miR-26a/b-5p mimics, miR-26a/b-5p inhibitor or sh-YKL-40 were transduced into EC cells. All lentiviruses were packaged by Ribobio (Guangzhou, China). Lentivirus transduction was performed in starving medium containing 8 μg/ml polybrene. To obtain stable cell lines, antibiotic-based clone selection was performed 72 h later with the use of 1 μg/ml puromycin for 3 weeks.

To overexpress STAT3 in EC cells, the STAT3 expression plasmid (Cat: HG10034-NM, Sino Biological, Beijing, China) was transfected into EC cells using Lipofectamine 2000 (Thermo Fisher, Waltham, MA, USA). After 6 h, the starving medium was replaced by full medium and selection was continued on with 200 μg/ml hygromycin for 4 weeks.

Immunofluorescence

The isolated CAFs or NFs were fixed in 4% paraformaldehyde. After permeabilization in 0.2% Triton X-100 and blocking in goat serum, the cells were probed with primary antibodies α-SMA (1:500, bsm-33187M, Bioss, Beijing, China) and vimentin (1:100, bsm-0756R, Bioss) overnight at 4°C. Subsequently, Goat Anti-Mouse IgG/FITC (1:100, bs-0296G-FITC, Bioss) and Goat Anti-rabbit IgG/Cy3 (1:100, bs-0295G-Cy3, Bioss) were applied. After nuclear counterstaining with DAPI, the cells were observed using a fluorescent microscope (Olympus, Tokyo, Japan).

Exosome isolation and characterization

Exosomes were isolated from the culture supernatants of CAFs or NFs using ExoQuick-TC Precipitation Solution (System Bioscience, Palo Alto, CA, USA). Briefly, the supernatants were pre-cleaned by successive centrifugations at 2000 g for 10 min and 10,000 g for 30 min and filtration through 0.22 μm filters. Subsequently, ultracentrifugation at 110, 000 g for 2 h was carried out for exosome collection. Then, the ExoQuick Solution was added to the media followed by centrifugation at 1500 g for 30 min. Afterwards, the exosomes were suspended in phosphate buffer solution. To characterize the isolated exosomes, the expression of CD63, CD81, Hsp70, TSG101, TFIIB, and LaminA/C was detected by Western blot analysis. Moreover, the expression of CD63 in exosomes was further verified by flow cytometry. The exosomes were incubated with CD63-Alexa647 antibody (BioLegend, San Diego, CA, USA) for 2 h followed by detection on a flow cytometer. To observe the presence and morphology of the prepared exosomes, transmission electron microscopy (TEM) was applied. In brief, the fixed exosomes were dropped onto copper grid, immersed in 2% phosphotungstic acid, dried for 10 min, and observed under the TEM (Hitachi, Tokyo, Japan) at 100 kV.

Exosome uptake

The exosomes were labeled by the fluorescent dye Dil (10 μM, Beyotime, Haimen, China). Then ultracentrifugation at 100,000 g for 1 h was performed to remove the residual dye. After washing for three times, the labeled exosomes were resuspended in phosphate buffer solution and added to HEC-1A and RL95-2 cells. Twenty-four hours later, the cells were washed with phosphate buffer solution and the uptake of exosomes was evaluated under a laser confocal microscopy (Olympus, Tokyo, Japan).

Co-culture assay

The co-culture of CAFs and EC cells was performed using a Transwell co-culture system. Briefly, EC cells and CAFs were cultured in the bottom well and upper well, respectively. The ratio of EC cells to CAFs was 1:3. After co-culture for 48 h, the EC cells were collected for further detection.

Real-time quantitative PCR analysis

Total RNA was isolated from tissue samples, cells, CAFs and NFs with TRIzol (Thermo Fisher), while exosomal RNA was isolated with the

Table 1

Oligonucleotide primer sets for RT-qPCR.

Name	Sequence (5′–3′)	Length
NEAT1 F	GTACGCGGGCAGACTAACAC	20
NEAT1 R	TGCGTCTAGACACCACAACC	20
YKL-40 F	ATCACCAAGGAGCCAAACATC	21
YKL-40 R	GGGGAAGTAGGATAGGGGACA	21
STAT3 F	TAGCAGGATGGCCCAATGGAATCA	24
STAT3 R	AGCTGTCACTGTAGAGCTGATGGA	24
miR-26a-5p F	UCCAUAAAGUAGGAAACACUACA	23
miR-26a-5p R	CAGUACUUUUGUGUAGUACAA	21
miR-26b-5p F	CCGGGACCCAGTTCAAGTAA	20
miR-26b-5p R	CCCCGAGCCAAGTAATGGAG	20
U6 F	GCTTCGGCAGCACATATACTAAAA	24
U6 R	CGCTTCACGAATTTGCGTGTCAT	23
β-actin F	ACACTGTGCCCATCTACG	18
β-actin R	TGTCACGCACGATTTCC	17

YKL-40, chitinase 3 like 1; NEAT1, nuclear enriched abundant transcript 1, STAT3, signal transducers and activators of transcription.

miRNeasy Mini Kit (Qiagen, Dusseldorf, Germany). Afterwards, the isolated RNA was converted into cDNA using the iscript cDNA synthesis kit (BIO-RAD, Hercules, CA, USA). SYBR Green Realtime PCR Master Mix (SinoBio, Shanghai, China) was used for Real-time RT-PCR analysis. The relative level of RNA normalized to β-actin or U6 snRNA was calculated using $2^{-\Delta\Delta Ct}$ method. The primer sequences are described in Table 1.

Western blot analysis

The protein samples were extracted from tissues, cells and exosomes using radio-immunoprecipitation assay buffer (Beyotime). Equal amount (25 μg) of protein was separated through SDS-PAGE and blotted onto polyvinylidene fluoride membranes (BIO-RAD). Then, blocking in 5% skim milk was carried out. Proteins were detected by incubation with appropriate primary antibodies TFIIB (1:500, A1708, ABclonal, Wuhan, China), LaminA/C (1:10000, A19524, ABclonal), CD63 (1:500, bs-0342R, Bioss), CD81 (1:500, bs-6934R, Bioss), Hsp70 (1:500, bs-0244R, Bioss), TSG101 (1:500, A5789, ABclonal), YKL-40 (1:500, bs-10215R, Bioss), STAT3 (1:1000, bs-52235R, Bioss), p-STAT3 (1:1000, bs-22386R, Bioss), Rab27a (1:500, A1934, ABclonal), β-actin (1:20000, AC026, ABclonal) overnight at 4°C coupled with HRP-conjugated Goat Anti-Rabbit secondary antibody (1:5000, AS063, ABclonal). ECL reagent (Solarbio, Beijing, China) was used for visualization of proteins.

Luciferase analysis

The interaction between NEAT1/STAT3 and miR-26a/b-5p was evaluated by luciferase analysis. Briefly, the HEC-1A and RL95-2 cells were transfected with the NEAT1/STAT3 reporter construct containing the wild type (WT) or mutant type (MUT) miR-26a/b-5p binding sites, together with miR-26a/b-5p mimics or inhibitor using Lipofectamine 2000. At 24 h after the transfection, the luciferase signals were detected using the Dual Luciferase Reporter Gene Assay Kit (Beyotime).

RIP assay

MS2-binding protein (MS2bp)-NEAT1/STAT3 (construct containing NEAT1/STAT3 transcript), MS2bs- NEAT1/STAT3 mt (the miR-26a/b-5p binding sites were mutated) or MS2bs-Rluc vector and MS2bp-GFP were co-transfected into HEC-1A and RL95-2 cells using Lipofectamine 2000. Forty-eight hours later, the HEC-1A cells were harvested, lysed and incubated with GFP antibody (ChromoTek, gtma-20, Munich, Germany). The RNA-protein complexes were treated with TRIzol and the miR-26a/b-5p level was detected by RT-qPCR.

Chromatin immunoprecipitation (ChIP)

The binding between p-STAT3 and the YKL-40 promoter region was verified by ChIP using a MagnaChIP kit (Millipore, Billerica, MA, USA). The cells with exosome treatment were subjected to cross-linking and lysed in RIPA. After receiving sonicate, cell lysates were immunoprecipitated with p-STAT3 (ab76315, Abcam, Cambridge, UK) or IgG antibody. The precipitated DNA-protein complexes were evaluated with RT-qPCR to quantify the p-STAT3 binding DNA.

MTT assay

EC cells were plated in 96-well plates, and MTT assay was performed to evaluate the growth of cells. After treatment with exosomes for 24, 48, and 72 h, MTT (20 nmol/L; Beyotime) was added and incubated at 37°C for 4 h. The absorbance of 490 nm was measured after adding with 150 μL DMSO.

Colony formation assay

The single cell suspension of EC cells was seeded into 6-well plates. The culture medium was changed every 3 d. After culture for 14 d, the cells were fixed in 4% paraformaldehyde for 20 min, stained in 0.2% crystal violet for 5 min, and then photographed.

Tumorigenicity assay in vivo

All animal experiments were performed in accordance with the NIH Guide for the Care and Use of Laboratory Animals and approved by the ethics committee of the First Affiliated Hospital of Guangxi Medical University. Female athymic BALB/c nude mice of six weeks old obtained from Hunan Slac Jingda Laboratory Animal Co., Ltd were used for subcutaneous xenograft study. HEC-1A cells (1×10^6) stably infected with lentivirus expressing miR-26a/b-5p or NC (HEC-1A, HEC-1A-NC, HEC-1A-miR-26a/b-5p mimics) either alone or mixed with CAFs (1×10^6) stably infected with lentivirus expressing sh-NC, sh-Rab27a, sh-NC, sh-NEAT1, vector, or NEAT1 (CAFs, CAFs-sh-NC, CAFs-sh-Rab27a, CAFs-sh-NC, CAFs-sh-NEAT1, CAFs-vector, CAFs-NEAT1) were subcutaneously injected into the nude mice. In order to suppress the release of exosomes, CAFs were treated with GW4869 (20 μM) before the subcutaneous injection. Subsequently, the mice were intraperitoneally injected with 2 mg/kg GW4869 at 72 h after the inoculation every other day until tumor collection. The length and width of tumors were measured every 5 days. The mice were euthanized at 35 days after the inoculation, and the tumors were collected for subsequent experiments.

Immunohistochemical analysis

The tumor tissues obtained from the nude mice were embedded in paraffin and cut into sections for immunohistochemistry analysis. After deparaffinization, rehydration, antigenic retrieval, blocking in goat serum, the sections were incubated with primary Ki-67 antibody (1:100, bs-23103R, Bioss) at 4°C overnight and developed with mouse anti-rabbit IgG/HRP (1:100, bs- 0295M-HRP, Bioss). The sections were subjected to counterstaining with hematoxylin, and detected under a microscopy. The number of Ki-67 positive cells was counted.

Statistical analysis

All data from three independent biological repeats are expressed as the mean ± standard deviation (SD). Statistical analysis was performed using

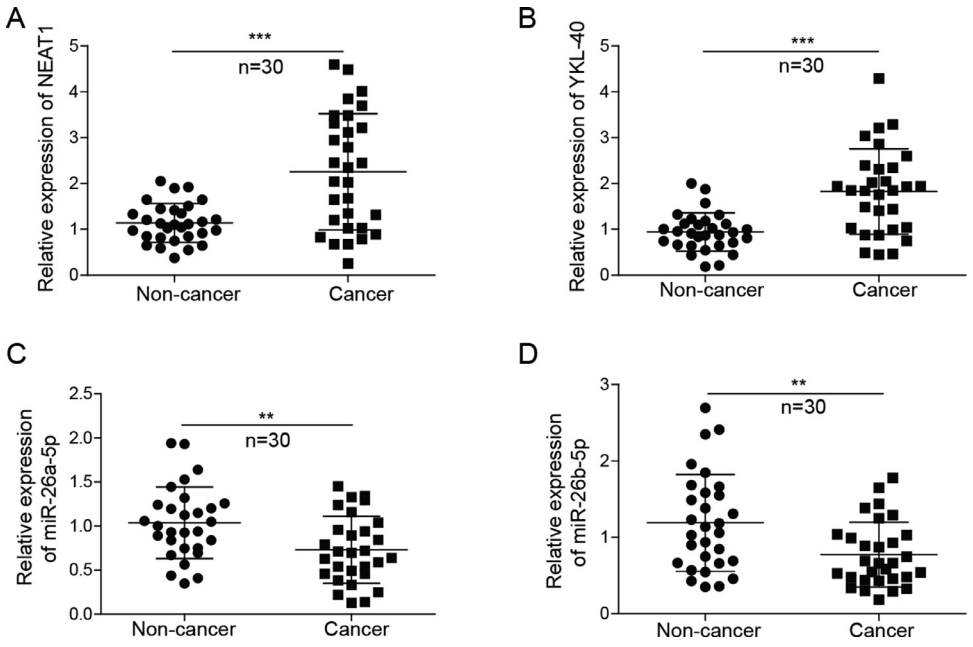

Fig. 1. Expression of NEAT1, YKL-40, and miR-26a/b-5p in human endometrial cancer. RT-qPCR analysis of NEAT1(A), YKL-40(B), and miR-26a/b-5p (C, D) levels in endometrial cancer and normal endometrial tissues. All data were shown as mean ± SD (n = 30). **, $P < 0.01$; ***, $P < 0.001$.

GraphPad Prism software 8.0 (GraphPad Software Inc., La Jolla, CA, USA). Either Student's t test (between two groups) or one-way ANOVA with Bonferroni post hoc analysis (more than 2 groups) was used. $P < 0.05$ was considered statistically significant.

Results

Expression of NEAT1, YKL-40, and miR-26a/b-5p in patients with EC

As a first step toward uncovering the effect of NEAT1-miR-26-a/b-5p-YKL-40 axis on EC, RT-qPCR was used to assess the differential expression of NEAT1, YKL-40, and miR-26a/b-5p in 30 EC and normal endometrial specimens. A significant up-regulation of NEAT1 and YKL-40 expression was found in EC tissues, compared with that in normal endometrial tissues. Conversely, miR-26a-5p and miR-26b-5p levels were down-regulated in EC patients (Fig. 1A-D). The primary transcripts of DNA transcription will undergo RNA processing to become the mature RNA. Therefore, we further detected the level of NEAT1 primary transcripts. However, there was no significant change in the level of NEAT1 primary transcripts between EC and normal endometrial tissues (Fig. S1A). Moreover, the expression levels of NEAT1, YKL-40, and miR-26a/b-5p in EC were analyzed using the TCGA data base. As shown in Fig. S2, miR-26a-5p level was down-regulated, while YKL-40 was up-regulated in EC patients. The levels of NEAT1 and miR-26b-5p were not different between EC and normal endometrial tissues. Thus, we speculated that exosomes-derived NEAT1 might contribute to the up-regulation of NEAT1 in EC. In addition, the differential expression of NEAT1-miR-26-a/b-5p-YKL-40 axis suggests its potential function in EC.

Exosomal NEAT1 derived from CAFs promotes STAT3 and YKL-40 expression in HEC-1A and RL95-2 cells

Next, primary CAFs and NFs were isolated from EC tissues and normal endometrial tissues, respectively. The expression of specific fibroblast markers α-SMA and vimentin was detected by immunofluorescent assay. As shown in Fig. 2A, the levels of α-SMA and vimentin in CAFs were higher than that in NFs. Moreover, the exosomes collected from the supernatant of CAFs and NFs were observed by TEM. As presented in Fig. 2B, the results indicated that vesicles were about 30-100 nm in diameter, and there were more exosomes released from CAFs than NFs. Flow cytometry further verified the presence of CD63, an exosome marker (Fig. 2C). Western blot analysis showed that nuclear proteins TFIIB and LaminA/C were not detected in exosomes and only expressed in CAFs. On the contrary, exosome markers CD63, CD81, Hsp70 and TSG101 proteins were expressed in exosomes (Fig. 2D). To examine exosome uptake by EC cells, the CAF-derived exosomes were labeled with Dil and added to EC cells. After incubation for 24 h, we found the intracellular localization of Dil-labeled exosomes (Fig. 2E).

The expression of NEAT1 in exosomes derived from paired CAFs and NFs was assessed by RT-qPCR. Remarkably, a higher expression level of NEAT1 was found in CAFs-derived exosomes compared with the paired NF-derived exosomes (Fig. 2F). Furtherly, after EC cells were incubated with the isolated exosomes for 48 h, incubation with CAFs-derived exosomes led to an increase in NEAT1 level in EC cells (Fig. 2G). Interestingly, the mRNA and protein levels of YKL-40 in EC cells were up-regulated after incubation with CAFs-derived exosomes for 48 h (Fig. 2H and I). In addition, the expression of NEAT1 in NFs, CAFs, normal endometrial epithelial cell lines, and EC cell lines (HEC-1A, HEC-1B, and RL95-2) was further determined. As shown in Fig. 3A, as compared with NFs or normal endometrial epithelial cells, endogenous NEAT1 level was remarkably raised in CAFs or EC cells.

To further assess the transfer of NEAT1 from CAFs to EC cells, the conditioned medium (CM) and exosome-depleted CM of CAFs were collected and added to EC cells. We observed that NEAT1 expression was increased by CAFs-CM treatment, which was significantly reduced when exosomes were depleted or treatment with GW4869, an inhibitor of exosome release (Fig. 3B and C). Moreover, after co-culture with CAFs for 48 h, EC cells expressed a higher level of NEAT1, whereas NEAT1 level was reduced when CAFs were treated with GW4869 (Fig. 3D). Accordingly, the protein levels of p-STAT3, STAT3 and YKL-40 were up-regulated by incubation with CAFs-CM or co-culture with CAFs, which were reversed by GW4869

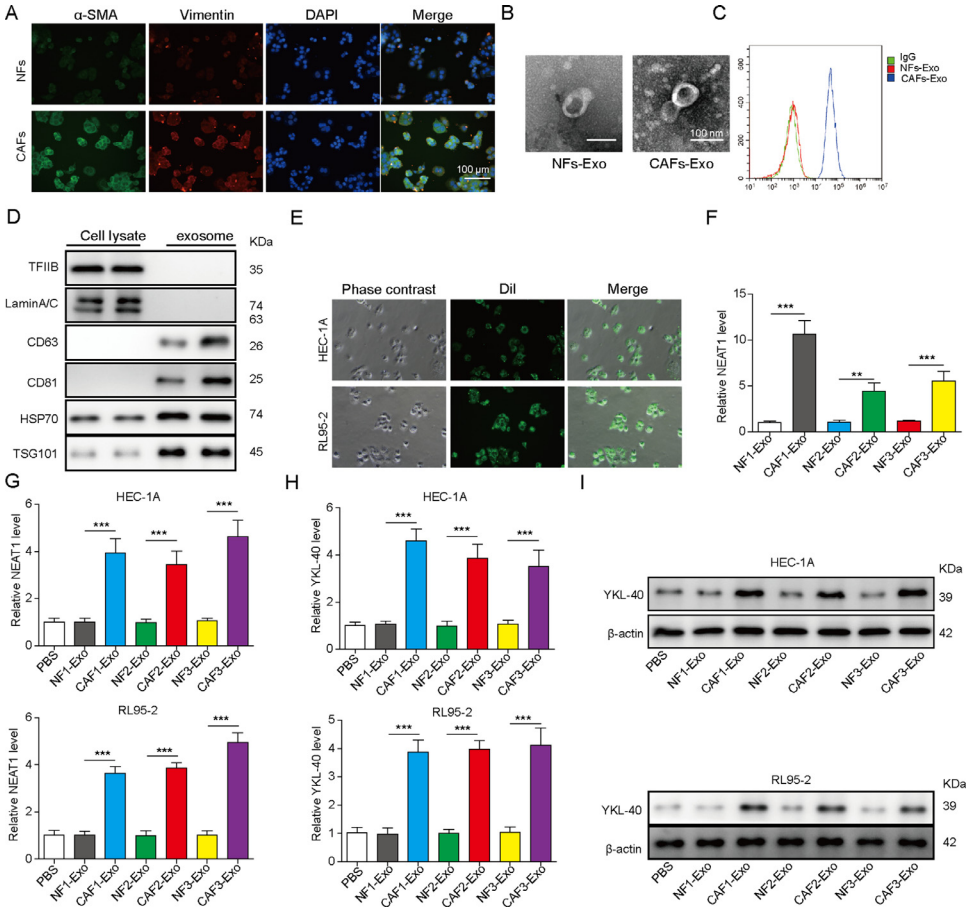

Fig. 2. CAF-derived exosomes promote YKL-40 expression in HEC-1A and RL95-2 cells. (A) Immunofluorescence assay for detection of α-SMA and vimentin expression in NFs and CAFs. Scale bar, 100 μm. (B) The morphology of exosomes was observed by transmission electron microscopy. (C) Flow cytometry for evaluating CD63 expression in exosomes. (D) Western blot analysis of TFIIB, LaminA/C, CD63, CD81, Hsp70, and TSG101 protein levels in CAF lysate and exosomes. (E) The green exosome fluorescence in HEC-1A and RL95-2 cells after incubation with Dil-labeled exosomes (10 μM) for 24 h was observed under a laser confocal microscopy. (F) RT-qPCR analysis of NEAT1 expression in the exosomes derived from three paired NFs and CAFs. HEC-1A and RL95-2 cells were incubated with PBS, or exosomes isolated from three paired NFs and CAFs for 48 h. (G) NEAT1 expression in EC cells was detected by RT-qPCR. (H) & (I) RT-qPCR and Western blot assays for determining YKL-40 expression in HEC-1A and RL95-2 cells. All data from three independent experiments were shown as mean ± SD (n = 6). **, $P < 0.01$; ***, $P < 0.001$.

administration (Fig. 3E and F). In addition, CAFs were infected with lentivirus expressing si-Rab27a to inhibit exosome release. The interference efficiency of si-Rab27a was verified by Western blot (Fig. 3G). As expected, CAFs-CM or co-culture with CAFs-mediated the increased expression of NEAT1 in EC cells was suppressed by silencing of Rab27a (Fig. 3H and I). Consistently, treatment with CM of Rab27a-silenced CAFs or co-culture with Rab27a-silenced CAFs resulted in decreased protein levels of p-STAT3, STAT3 and YKL-40 in EC cells (Fig. 3J and K). Next, the NEAT1 level in exosomes derived from CAFs with NEAT1 overexpression was raised, but reduced in exosomes from NEAT1-silenced CAFs (Fig. 3L). The intracellular NEAT1 level was up-regulated by incubation with exosomes from NEAT1-overexpressed CAFs, but down-regulated when NEAT1 was knocked down in CAFs (Fig. 3M). Moreover, incubation with exosomes derived from NEAT1-silenced CAFs led to decrease in mRNA and protein levels of STAT3, p-STAT3 and YKL-40 in EC cells. However, we got opposite results when NEAT1 was overexpressed in CAFs (Fig. 3N and O). As shown in Fig. 3P and Q, the growth of EC cells was promoted by incubation with CAFs-derived exosomes. Exosomes derived from NEAT1-silenced CAFs led to inhibition in growth, however, we got opposite results from NEAT1-overexpressed CAFs group. Furthermore, the inhibition in growth of EC cells induced by exosomes derived from NEAT1-silenced CAFs could be partly reversed by miR-26a/b-5p inhibitor or overexpression of STAT3 (Fig. S3A and B). Collectively, these results suggested that NEAT1 was transferred from CAFs to EC cells via exosomes, which subsequently promoted STAT3 and YKL-40 expression, and growth of EC cells.

Exosomal NEAT1 enhances YKL-40 expression via targeting miR-26a/b-5p

To further investigate the regulatory mechanisms of exosomal NEAT1 on YKL-40 expression, we focused on a series of miRNAs based on dbDEMC 2.0 database containing miRNA microarray in endometrial carcinoma and StarBase database for the prediction of target binding. Next, RT-qPCR was used to determine the expression changes of these screened miRNAs after silencing of NEAT1 in HEC-1A cells. According to the results, miR-26a/b-5p levels were the highest in NEAT1-silenced HEC-1A cells, compared with other candidate miRNAs, and therefore miR-26a/b-5p were selected in this study (Fig. S1B). Additionally, the expression changes of miR-26a/b-5p in CAFs-derived exosomes were not evident (Fig. S1C). As presented in Fig. 4A, there was no significant change in the level of miR-26a/b-5p in

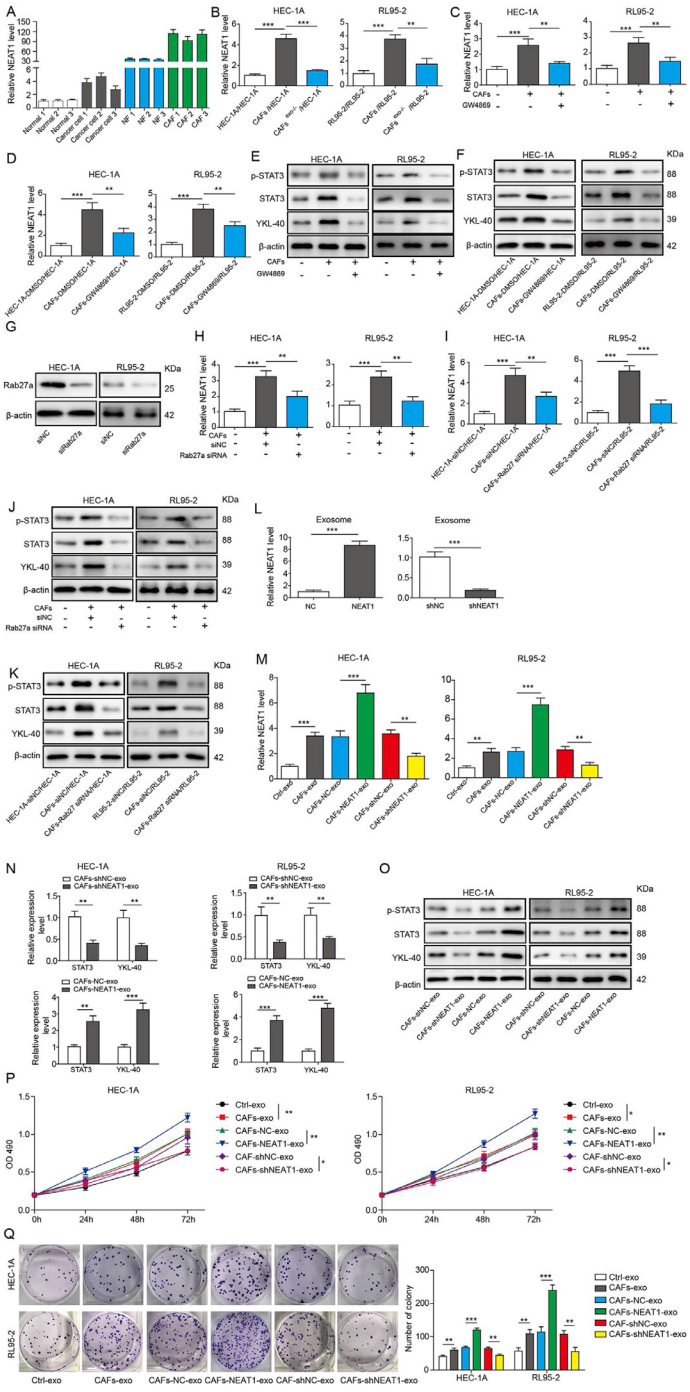

Fig. 3. Exosomal transfer of NEAT1 to EC cells leads to increased expression of STAT3 and YKL-40. (A) RT-qPCR analysis of NEAT1 expression level in NFs, CAFs, normal endometrial epithelial cells, and EC cells. (B) HEC-1A and RL95-2 cells were cultured in control CM, CAFs-CM, or exosome-depleted CAFs-CM for 48 h, then NEAT1 level was assessed by RT-qPCR. HEC-1A and RL95-2 cells were maintained in control CM, CAFs-CM, or 20 μM GW4869-treated CAFs-CM for 48 h. (C) NEAT1 expression was determined by RT-qPCR. (D) The NEAT1 level was assessed by RT-qPCR. (E) STAT3, p-STAT3 and YKL-40 levels were assessed by Western blot. HEC-1A and RL95-2 cells were co-cultured with CAFs or GW4869-treated CAFs for 48 h. (F) Western blot analysis of STAT3, p-STAT3, and YKL-40 levels. (G) Western blot analysis of Rab27a protein level in CAFs infected with lentivirus expressing si-NC or si-Rab27a. (H) HEC-1A and RL95-2 cells were cultured in control CM, CAFs-CM, or Rab27a-silenced CAFs-CM for 48 h, then NEAT1 level was detected by RT-qPCR. (I) HEC-1A cells and RL95-2 were co-cultured with CAFs or Rab27a-silenced CAFs for 48 h, and NEAT1 level was detected by RT-qPCR. (J)&(K) Protein levels of STAT3, p-STAT3, and YKL-40 were assessed by Western blot. (L) RT-qPCR analysis of NEAT1 level in exosomes isolated from CAFs infected with lentivirus expressing sh-NEAT1 or NEAT1 gene. (M) HEC-1A and RL95-2 cells were incubated with exosomes derived from CAFs, NEAT1-overexpressed CAFs, or NEAT1-silenced CAFs for 48 h. RT-qPCR was performed to assess NEAT1 level. (N)&(O) STAT3 and YKL-40 expression was detected by RT-qPCR and Western blot assays. (P) The proliferation of HEC-1A and RL95-2 cells was detected by MTT assay. (Q) The growth of HEC-1A and RL95-2 cells was evaluated by colony formation assay. All data from three independent experiments were shown as mean ± SD (n = 6). *, $P < 0.05$; **, $P < 0.01$; ***, $P < 0.001$.

exosomes derived from NEAT1-overexpressed or-silenced CAFs. Therefore, exosomal miR-26a/b-5p may have barely effects on EC cells. Whereas, we found a decrease in miR-26a/b-5p level in EC cells co-cultured with NEAT1-overexpressed CAFs. On the contrary, miR-26a/b-5p level was raised in EC cells after co-culture with NEAT1-knockdown CAFs (Fig. 4B). In addition, RT-qPCR results revealed that miR-26a/b-5p was overexpressed or depleted in HEC-1A and RL95-2 cells by infection with miR-26a/b-5p mimics or inhibitor (Fig. 4C). The protein level of YKL-40 in HEC-1A and RL95-2 cells was markedly reduced by miR-26a/b-5p overexpression, but improved by miR-26a/b-5p depletion (Fig. 4D). Bioinformatic analysis of Starbase database showed that NEAT1 had miR-26a/b-5p binding sites (Fig. 4E). To further investigate the interaction between NEAT1 and miR-26a/b-5p, luciferase analysis was performed in EC cells. Transfection with miR-26a/b-5p mimics caused the attenuation in the luciferase activity of WT but not MUT NEAT1 group. However, transfection with miR-26a/b-5p inhibitor presented the opposite results (Fig. 4F). Furthermore, RIP assay demonstrated that miR-26a/b-5p was obviously enriched in RNAs retrieved from MS2bs-NEAT1, but not MS2bs-NEAT1 mt with mutated miR-26a/b-5p binding sites (Fig. 4G). We then evaluated whether NEAT1 regulated STAT3 and YKL-40 expression through miR-26a/b-5p. Our data revealed that overexpression of miR-26a/b-5p reduced the protein levels of STAT3 and YKL-40. Moreover, the increased protein levels of STAT3 and YKL-40 induced by exosomes from NEAT1-overexpressed CAFs were counteracted by miR-26a/b-5p overexpression (Fig. 4H and I). Therefore, these data indicated that exosomal NEAT1 promoted STAT3 and YKL-40 expression via sponging miR-26a/b-5p.

MiR-26a/b-5p regulates YKL-40 expression via targeting STAT3

To further elucidate whether STAT3 was a target gene regulated by miR-26a/b-5p, luciferase analysis and RIP assay were carried out. As presented in Fig. 5A, there are two predicted binding sites between miR-26a/b-5p and STAT3 3'UTR. The luciferase analysis showed that ectopic expression of miR-26a/b-5p suppressed the luciferase activity of WT, MUT1 (only binding site 1 was mutated) and MUT2(only binding site 2 was mutated), but not MUT1&2 (both binding site 1 and 2 were mutated) STAT3 3′-UTR (Fig. 5B). Further RIP assay revealed that miR-26a/b-5p was highly enriched in RNAs retrieved from MS2bs-STAT3 3'UTR, compared with MS2bs-Rluc vector or mutant MS2bs-STAT3 3'UTR group (Fig. 5C). We further performed experiments to verify whether miR-26a/b-5p regulated YKL-40 expression via STAT3. Ectopic expression of STAT3 in HEC-1A and RL95-2 cells was confirmed by Western blot analysis (Fig. 5D). The mRNA and protein levels of YKL-40 were reduced by miR-26a/b-5p mimics, but improved by STAT3 overexpression. The reduction of STAT3 and YKL-40 expression induced by miR-26a/b-5p mimics was significantly reversed

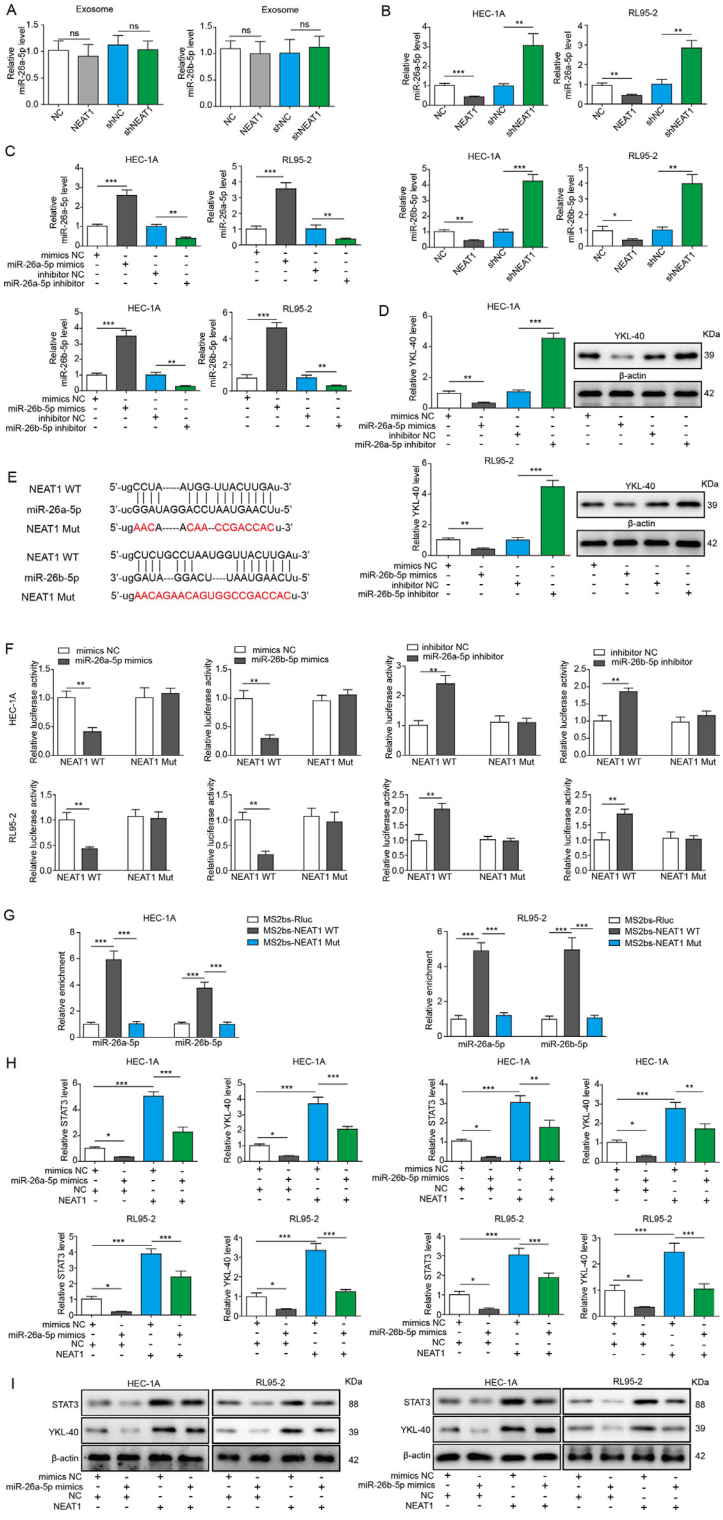

Fig. 4. Exosomal NEAT1 sponges miR-26a/b-5p to facilitate STAT3 and YKL-40 expression in EC cells. (A) RT-qPCR for miR-26a/b-5p level in exosomes derived from CAFs, NEAT1-overexpressed CAFs, or NEAT1-silenced CAFs. (B) HEC-1A and RL95-2 cells were co-cultured with NEAT1-overexpressed or silenced CAFs, and miR-26a/b-5p level was detected by RT-qPCR. (C) Expression of miR-26a/b-5p in HEC-1A and RL95-2 cells infected with lentivirus containing miR-26a/b-5p mimics or inhibitor was detected by RT-qPCR. (D) Expression of YKL-40 in HEC-1A and RL95-2 cells after overexpression or silencing of miR-26a/b-5p was assessed by Western blot. (E) The binding sites between NEAT1 and miR-26a/b-5p. Luciferase analysis (F) and RIP assay (G) was performed to determine interaction between NEAT1 and miR-26a/b-5p. The expression of STAT3 and YKL-40 in HEC-1A and RL95-2 cells received various treatments was assessed by RT-qPCR (H) and Western blot (I). All data from three independent experiments were shown as mean ± SD (n = 6). *, $P < 0.05$; **, $P < 0.01$; ***, $P < 0.001$, ns = no significant.

by STAT3 overexpression (Fig. 5E and F). In addition, we used JASPAR database to predict that p-STAT3 might bind to the promoter of YKL-40 (three binding sites, namely as BS1, BS2, and BS3) (Fig. 5G). Further ChIP and dual luciferase assays confirmed the direct binding between p-STAT3 and YKL-40 BS3 promoter (Fig. 5H and I). Thus, miR-26a/b-5p regulated YKL-40 expression via targeting STAT3.

Exosomal NEAT1-miR-26a/b-5p-YKL-40 axis regulates tumor growth in vivo

To evaluate whether exosomal NEAT1 derived from CAFs affected tumorigenicity in vivo via regulating miR-26a/b-5p-YKL-40 axis, a subcutaneous xenograft mode by injection of HEC-1A cells with or without CAFs was established. The tumor volume of mice injected with HEC-1A cells and CAFs was greater than that of HEC-1A group. Administration with GW4869 remarkably restrained CAFs-mediated tumor promotion (Fig. 6A). In addition, NEAT1 level in xenograft tissues was increased, while miR-26a/b-5p level was decreased after the injection with CAFs, which were weakened by GW4869 (Fig. 6B). As detected by immunohistochemical staining, the percentage of Ki-67-positive cells in xenograft tissues was enhanced in HEC-1A+CAFs group, whereas GW4869 treatment counteracted this effect (Fig. 6C). Western blot assay revealed that GW4869 suppressed CAFs-mediated increase in YKL-40 and STAT3 protein levels in tumor tissues (Fig. 6D). Consistent with the above results, knockdown of Rab27a in CAFs effectively reversed CAFs-induced increase in tumor volume, NEAT1 level, percentage of Ki-67-positive cells, and YKL-40, STAT3 protein levels, and decrease in miR-26a/b-5p level (Fig. 6E-H). Subsequently, we investigated the effect of exosomal NEAT1 on tumorigenicity *in vivo*. To achieve this, the nude mice were injected with HEC-1A cells with or without NEAT1-silenced/overexpressed-CAFs. According to the results, the increased tumor volume, NEAT1 level, Ki-67-positive cell number, and YKL-40, STAT3 levels, while the decreased miR-26a/b-5p level in CAFs group were significantly suppressed in NEAT1-silenced CAFs group, but further promoted in NEAT1-overexpressed CAFs group (Fig. 6I-L). Finally, to determine whether the exosomal NEAT1 affected *in vivo* tumor growth via miR-26a/b-5p, the nude mice were injected with miR-26a/b-5p-overexpressed HEC-1A cells with or without NEAT1-overexpressed-CAFs. As expected, overexpression of miR-26a/b-5p inhibited tumorigenicity as evidenced by decreased tumor volume and Ki-67 expression (Fig. 7A and B). Furthermore, the enhanced tumor volume and Ki-67 expression caused by NEAT1-overexpressed CAFs were counteracted by ectopic expression of miR-26a/b-5p (Fig. 7A and B). As shown in Fig. 7C, miR-26a/b-5p overexpression repressed STAT3 and YKL-40 levels in tumor tissues. NEAT1-overexpressed-CAFs injection led to increased STAT3 and YKL-40 levels, which were significantly reversed by miR-26a/b-5p overexpression. To validate the involvement of YKL-40 in exosomal NEAT1-mediated *in vivo* tumor growth, the nude mice were injected with YKL-40-depleted HEC-1A cells with or without NEAT1-overexpressed-CAFs. Western blotting confirmed the interference efficiency of YKL-40 (Fig. S4A). Notably, NEAT1-overexpressed CAFs-induced increase in tumor volume and Ki-67 expression was abolished by silencing of YKL-40 (Fig. S4B and C). The enhanced YKL-40 level in NEAT1-overexpressed-CAFs group was significantly restored by sh-YKL-40 (Fig. S4D). Taken together, these findings

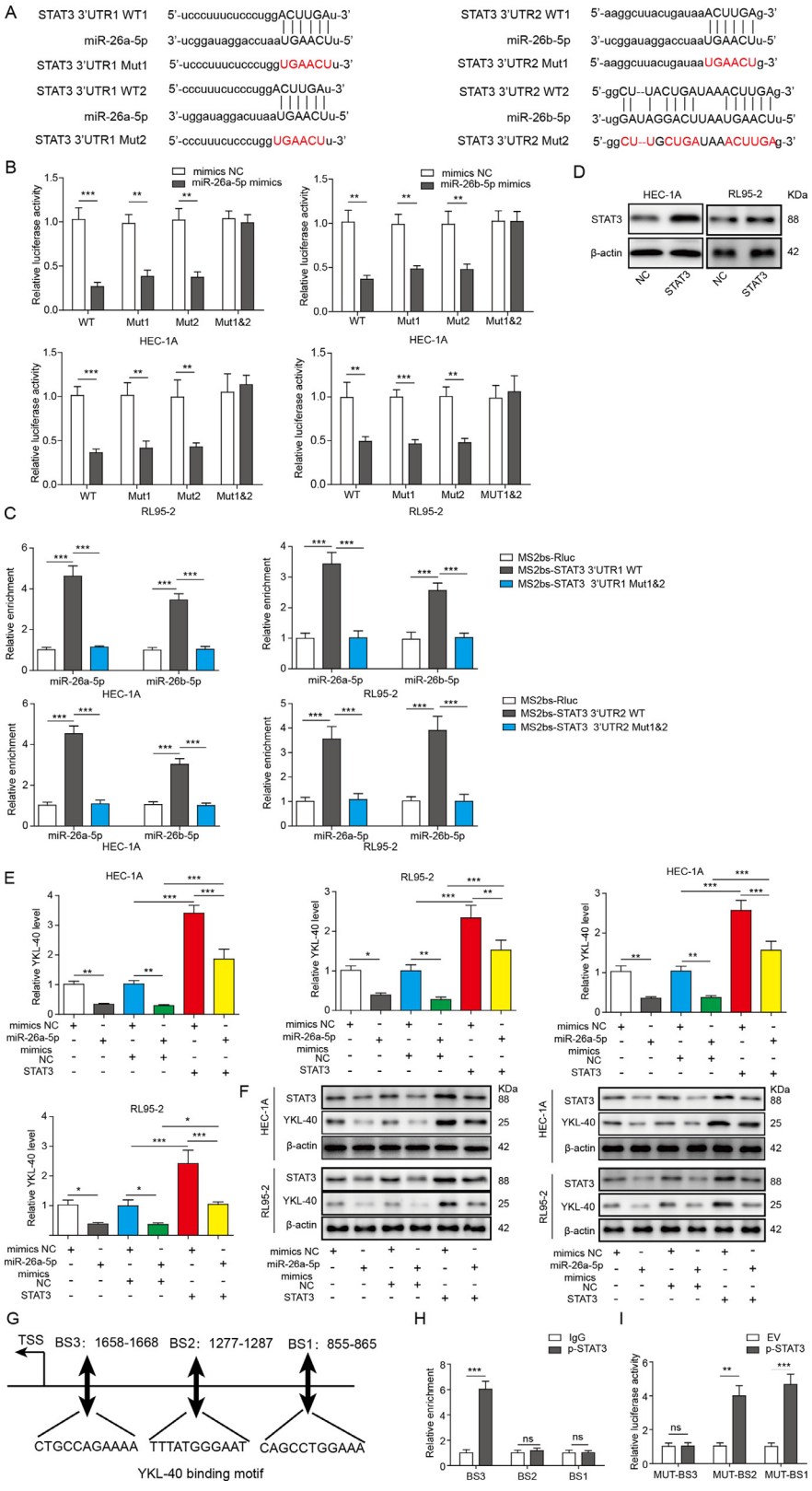

Fig. 5. MiR-26a/b-5p suppresses YKL-40 expression via targeting STAT3 in EC cells. (A) Two binding sites of miR-26a/b-5p to the 3'-UTR of STAT3. The interaction between STAT3 and miR-26a/b-5p was detected by luciferase analysis (B) and RIP assay (C). (D) The protein level of STAT3 in HEC-1A and RL95-2 cells after the transfection of STAT3 expression plasmid was assessed by Western blot. RT-qPCR (E) and Western blot (F) were used for determining YKL-40 and STAT3 expression in HEC-1A cells from various groups. (G) Three p-STAT3-binding sites (BS1, BS2, and BS3) at YKL-40 promoter were shown. (H) ChIP assay using anti-p-STAT3 antibody was used to verify the binding between p-STAT3 and the promoter of YKL-40 under exosome treatment. (I) The interaction between p-STAT3 and YKL-40 was assessed by the dual luciferase reporter assay. All data from three independent experiments were shown as mean ± SD (n = 6). **, $P < 0.01$; ***, $P < 0.001$, ns = no significant.

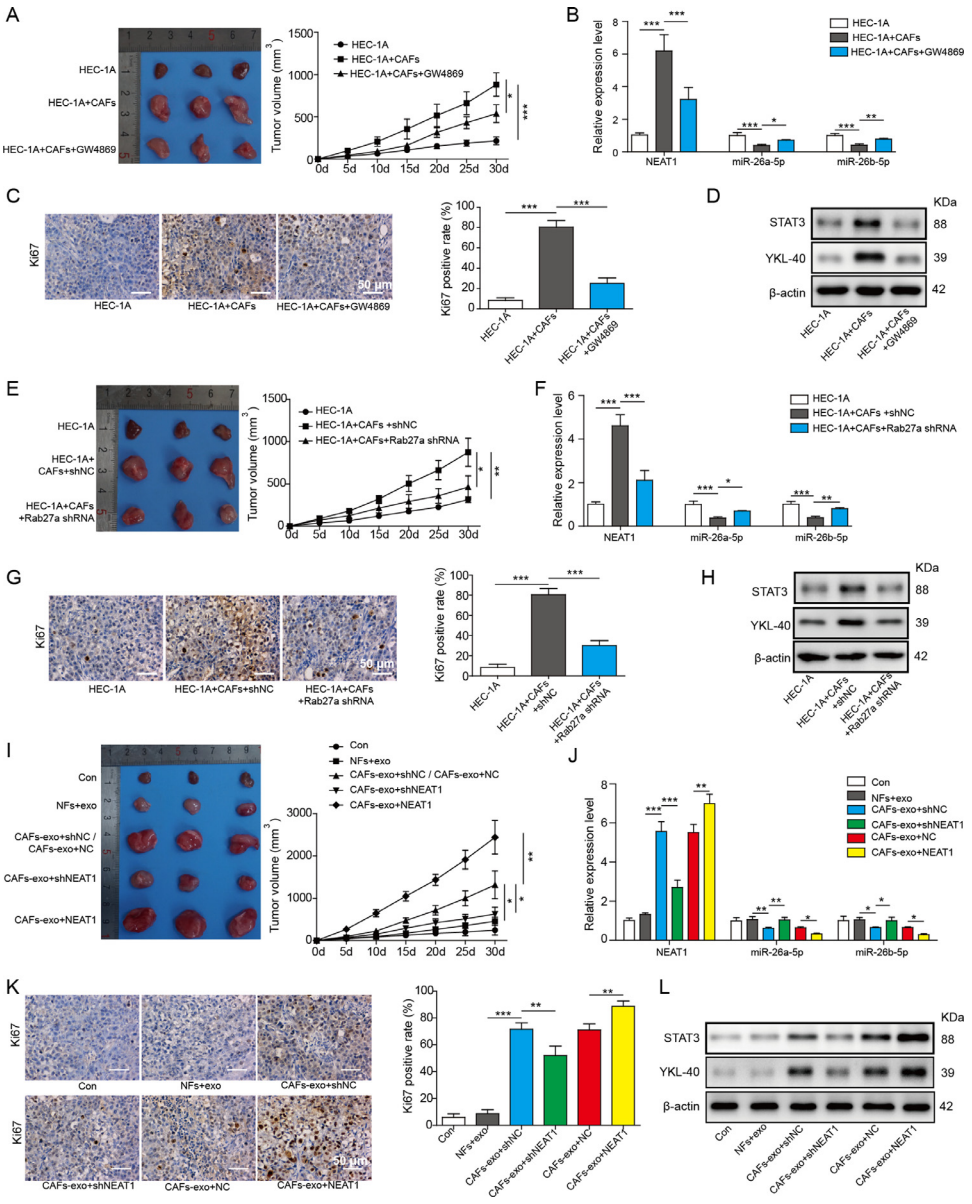

Fig. 6. CAFs-derived exosomal NEAT1 accelerates tumor growth in vivo via up-regulating YKL-40. Nude mice were subcutaneously injected with HEC-1A cells with or without CAFs. GW4869 (2 mg/kg) was intraperitoneally injected into the mice every other day. (A) The tumor growth curve was shown. (B) RT-qPCR analysis of NEAT1 and miR-26a/b-5p expression in tumor tissues. (C) Immunohistochemical staining for Ki-67 expression in tumor tissues. (D) Western blot analysis of YKL-40 and STAT3 protein level in tumor tissues. Nude mice were subcutaneously injected with HEC-1A cells with or without CAFs that were stably transfected with sh-NC or sh-Rab27a. (E) The tumor growth curve was shown. (F) RT-qPCR analysis of NEAT1 and miR-26a/b-5p expression in tumor tissues. (G) Immunohistochemical staining for Ki-67 expression in tumor tissues. (H) Western blot analysis of YKL-40 and STAT3 protein level in tumor tissues. HEC-1A cells with or without CAFs stably transfected with sh-NEAT1 or NEAT1 gene were subcutaneously injected into the nude mice. (I) The tumor growth curve was shown. (J) RT-qPCR analysis of NEAT1 and miR-26a/b-5p expression in tumor tissues. (K) Immunohistochemical staining for Ki-67 expression in tumor tissues. (L) Western blot analysis of YKL-40 and STAT3 protein levels in tumor tissues. All data from three independent experiments were shown as mean ± SD (n = 6). *, $P < 0.05$; **, $P < 0.01$; ***, $P < 0.001$.

revealed that exosomal NEAT1 derived from CAFs promoted tumorigenicity *in vivo* via regulating miR-26a/b-5p-YKL-40 axis.

Discussion

Tumor microenvironment, a complicated and dynamic network of intercellular communications, plays critical roles in tumor initiation and development [19]. CAFs are the major constituent of tumor microenvironment, which promote cancer growth and metastasis via exosomes [20,21]. Therefore, uncovering the regulatory mechanisms between cancer and CAFs mediated by exosomes is critical to develop anti-tumor strategy. Although lncRNA NEAT1 has been identified to be upregulated and promote the progression of EC; little is known about whether NEAT1 is present in the circulating CAFs-exosomes and its potential mechanisms and roles in EC. In this study, we verified for the first time that the level of exosomal NEAT1 released from CAFs was increased in EC, as

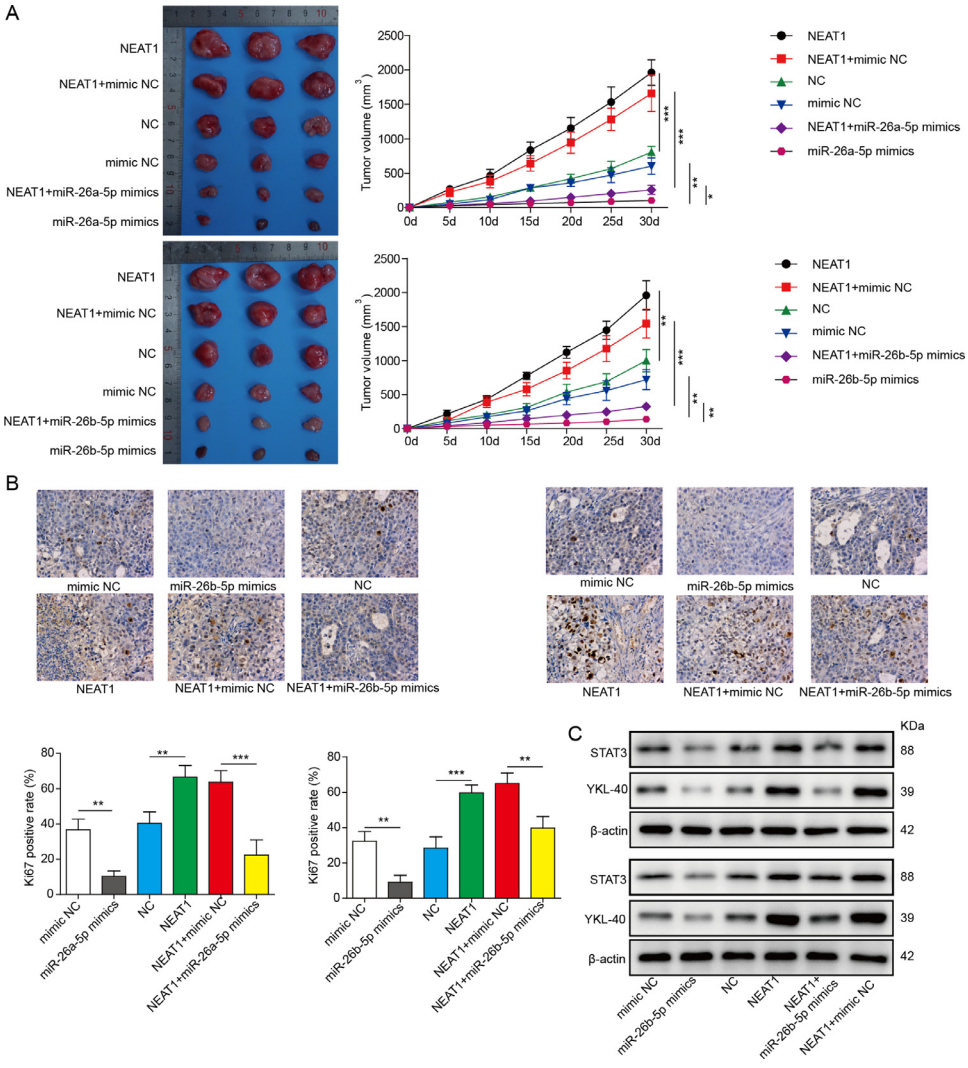

Fig. 7. Overexpression of miR-26a/b-5p reverses exosomal NEAT1-mediated protumorigenic effect *in vivo*. HEC-1A cells stably transfected with miR-26a/b-5p mimics or NC mimics were mixed with or without CAFs stably expressing NC vector or NEAT1, which were subcutaneously injected into the nude mice. (A) The tumor growth curve was shown. (B) Immunohistochemical staining for Ki-67 expression in tumor tissues. (C) Western blot analysis of YKL-40 and STAT3 protein levels in tumor tissues. All data from three independent experiments were shown as mean ± SD (n = 6). *, $P < 0.05$; **, $P < 0.01$; ***, $P < 0.001$.

compared with that in NFs. In addition, the results showed that NEAT1 was transferred from CAFs to HEC-1A and RL95-2 cells via exosomes, which improved the level of YKL-40, a recognized biomarker of EC. Moreover, we demonstrated that miR-26a/b-5p was a target of exosomal NEAT1, and implicated in exosomal NEAT1-mediated YKL-40 regulation. Furthermore, miR-26a/b-5p regulated YKL-40 expression via targeting STAT3. Finally, exosomal NEAT1 promoted tumorigenicity *in vivo* via regulating miR-26a/b-5p-STAT3-YKL-40 axis.

First, we determined the expression levels of NEAT1, YKL-40, and miR-26a/b-5p in 30 EC and normal endometrial specimens. Up-regulation of NEAT1 and YKL-40, but down-regulation of miR-26a/b-5p was found in EC patients. However, according to TCGA data base (http://www.cbioportal. org), NEAT1 and miR-26b-5p levels did not show any significant difference between EC and normal endometrial tissues. This discrepancy is most likely due to the difference in sample size. Since no difference in NEAT1 expression, the contribution of NEAT1 to EC progression might be through other mechanisms, such as exosomes-mediated delivery of NEAT1 to EC cells.

It has been documented that CAFs affect the tumorigenic phenotypes via releasing exosomes into the microenvironment [21]. Even worse, the released exosomes could lead to malignant behaviors in remote organs through body fluid circulation [22]. Increasing evidence demonstrates that exosomes promote oncogenesis via spreading tumor-promoting molecules, including DNAs, proteins, and non-coding RNAs [23,24]. The protumorigenic effects of exosomal lncRNAs have been verified. For example, exosomal lncRNA H19 could move to sensitive cells and increase the doxorubicin resistance in breast cancer [25]; lncRNA UCA1 enriched in exosomes contributed to bladder tumor growth and development and could be served as a diagnostic marker [26]. Currently, the roles of exosomal lncRNAs in EC have not been documented. In our study, we found that the NEAT1 level was higher in CAF-exosomes than in NFs-exosomes. Importantly, we first discovered the transfer of exosomal NEAT1 derived from CAFs to HEC-1A and RL95-2 cells. It has been recognized that lncRNAs may regulate gene expression via multiple complicated mechanisms [27]. So far, the detailed mechanisms of NEAT1 in EC have not been clarified. Previous studies have reported that YKL-40 contributed to the progression of EC

and might be a prognostic indicator for EC [8,28,29]. In the present study, the results revealed that exosomal NEAT1 promoted YKL-40 expression in recipient HEC-1A and RL95-2 cells, however GW4869 or si-Rab27a-mediated suppression of exosome release reversed this result. We also found that YKL-40 expression was increased by exosomes derived from NEAT1-overexpressed CAFs, but reduced by exosomes derived from NEAT1-silenced CAFs. These findings indicated the potential roles of internalized exosomal NEAT1 in the development of EC via regulating YKL-40.

As a research hotspot, the interaction between lncRNAs and mRNAs and their potential mechanisms have been widely concerned. Competing endogenous RNAs (ceRNAs) was first hypothesized by Salmena et al., suggesting the cross-talk between lncRNAs and mRNAs through competitively binding to miRNAs [30]. Luo et al. indicated that NEAT1 served as a ceRNA to accelerate colorectal cancer development via modulating miRNA-34a-SIRT1 axis [31]. LncRNA LINC00336 was reported to function as a ceRNA to promote lung cancer growth via inhibiting ferroptosis [32]. In this study, we identified that both NEAT1 and STAT3 3'UTR could bind to miR-26a/b-5p. Hence, we speculated that exosomal NEAT1 might affect EC progression through a ceRNA network. Further luciferase analysis and RIP assay verified that NEAT1 and STAT3 3'UTR could directly interact with miR-26a/b-5p. As demonstrated by a previous study, STAT3 could activate the transcription of YKL-40 [9]. Thus, we further guessed that the exosomal NEAT1 might regulate YKL-40 expression via miR-26a/b-5p-STAT3 axis. Our results verified this speculation and showed that miR-26a/b-5p level was down-regulated by exosomes from NEAT1-overexpressed CAFs, while up-regulated by exosomes from NEAT1-depleted CAFs. In addition, miR-26a/b-5p overexpression inhibited STAT3 and YKL-40 expression, which was counteracted by exosomal NEAT1. Overexpression of STAT3 suppressed miR-26a/b-5p mimics-induced down-regulation of YKL-40 level in HEC-1A and RL95-2 cells. In consistent with the *in vitro* results, exosomal NEAT1 conferred in vivo tumor growth via miR-26a/b-5p-STAT3-YKL-40 axis. These observations revealed that exosomal NEAT1 derived from CAFs promoted EC progression via miR-26a/b-5p-STAT3-YKL-40 axis.

Taken together, NEAT1 within exosomes released by CAFs can activate STAT3 via sponging miR-26a/b-5p, thus enhancing downstream YKL-40 expression in the recipient HEC-1A and RL95-2 cells. This mechanism of exosomal NEAT1 participates in the crosstalk in the tumor microenvironment, which confers the development of EC. Our study deeply explores the mechanisms of the malignant process of EC, as well as provides evidence for CAFs, NEAT1, or miR-26a/b-5p-STAT3-YKL-40 axis as therapeutic targets for EC.

Conflict of Interest

The authors declare no potential conflicts of interest.

Acknowledgments

This work was supported by grant from National Natural Science Foundation of China (No. 81960464) and Guangxi Natural Science Foundation (No. 2018GXNSFAA050146).

Ethics statement

Ethical approval was acquired from Ethics committee of the First Affiliated Hospital of Guangxi Medical University. Written informed consent was obtained from all patients.

All animal experiments were performed in accordance with the NIH Guide for the Care and Use of Laboratory Animals and approved by the ethics committee of the First Affiliated Hospital of Guangxi Medical University.

Data statement

All data generated or analyzed during this study are included in this published article

Author Contributions

Conceptualization: Jiang-Tao Fan; Data curation: Qin Luo; Formal analysis:Qin Luo; Funding acquisition: Zhao-Yu Zhou; Investigation:Zhao-Yu Zhou, Yan-Lu Luo; Methodology: Qin Luo; Project administration: Jiang-Tao Fan; Resources: Si-Bang Chen; Software: Si-Bang Chen; Supervision: Jiang-Tao Fan; Validation: Qiao-Ru Chen; Visualization: Zhao-Yu Zhou; Roles/Writing - original draft: Jin-Che Zhao; Writing - review & editing: Jiang-Tao Fan.

Supplementary materials

Supplementary material associated with this article can be found, in the online version, at doi:10.1016/j.neo.2021.05.004.

References

[1] Siegel RL, Miller KD, Jemal A. Cancer statistics, 2019. *CA Cancer J Clin* 2019;**69**:7–34.

[2] Lortet-Tieulent J, Ferlay J, Bray F, Jemal A. International Patterns and Trends in Endometrial Cancer Incidence, 1978-2013. *J Natl Cancer Inst* 2018;**110**:354–61.

[3] Siegel RL, Miller KD, Jemal A. Cancer statistics, 2015. *CA Cancer J Clin* 2015;**65**:5–29.

[4] Bian B, Li L, Yang J, Liu Y, Xie G, Zheng Y, Zeng L, Zeng J, Shen L. Prognostic value of YKL-40 in solid tumors: a meta-analysis of 41 cohort studies. *Cancer Cell Int* 2019;**19**:259.

[5] Rusak A, Jablonska K, Dziegiel P. The role of YKL-40 in a cancerous process. *Postepy Hig Med Dosw (Online)* 2016;**70**:1286–99.

[6] Fan JT, Si XH, Liao Y, Shen P. The diagnostic and prognostic value of serum YKL-40 in endometrial cancer. *Arch Gynecol Obstet* 2013;**287**:111–15.

[7] Peng C, Peng J, Jiang L, You Q, Zheng J, Ning X. YKL-40 protein levels and clinical outcome of human endometrial cancer. *J Int Med Res* 2010;**38**:1448–57.

[8] Li L, Fan J, Li D, Liu Y, Shrestha P, Zhong C, Xia X, Huang X. Influence of YKL-40 gene RNA interference on the biological behaviors of endometrial cancer HEC-1A cells. *Oncol Lett* 2018;**16**:1777–84.

[9] Singh SK, Bhardwaj R, Wilczynska KM, Dumur CI, Kordula T. A complex of nuclear factor I-X3 and STAT3 regulates astrocyte and glioma migration through the secreted glycoprotein YKL-40. *J Biol Chem* 2011;**286**:39893–903.

[10] Miyamoto K, Seki N, Matsushita R, Yonemori M, Yoshino H, Nakagawa M, Enokida H. Tumour-suppressive miRNA-26a-5p and miR-26b-5p inhibit cell aggressiveness by regulating PLOD2 in bladder cancer. *Br J Cancer* 2016;**115**:354–63.

[11] Li Y, Sun Z, Liu B, Shan Y, Zhao L, Jia L. Tumor-suppressive miR-26a and miR-26b inhibit cell aggressiveness by regulating FUT4 in colorectal cancer. *Cell Death Dis* 2017;**8**:e2892.

[12] Li J, Liang Y, Lv H, Meng H, Xiong G, Guan X, Chen X, Bai Y, Wang K. miR-26a and miR-26b inhibit esophageal squamous cancer cell proliferation through suppression of c-MYC pathway. *Gene* 2017;**625**:1–9.

[13] Sun Z, Yang S, Zhou Q, Wang G, Song J, Li Z, Zhang Z, Xu J, Xia K, Chang Y, et al. Emerging role of exosome-derived long non-coding RNAs in tumor microenvironment. *Mol Cancer* 2018;**17**:82.

[14] Zhang H, Deng T, Liu R, Ning T, Yang H, Liu D, Zhang Q, Lin D, Ge S, Bai M, et al. CAF secreted miR-522 suppresses ferroptosis and promotes acquired chemo-resistance in gastric cancer. *Mol Cancer* 2020;**19**:43.

[15] Li BL, Lu W, Qu JJ, Ye L, Du GQ, Wan XP. Loss of exosomal miR-148b from cancer-associated fibroblasts promotes endometrial cancer cell invasion and cancer metastasis. *J Cell Physiol* 2019;**234**:2943–53.

[16] Wang W, Ge L, Xu XJ, Yang T, Yuan Y, Ma XL, Zhang XH. LncRNA NEAT1 promotes endometrial cancer cell proliferation, migration and invasion by regulating the miR-144-3p/EZH2 axis. *Radiol Oncol* 2019;**53**:434–42.

[17] Dong P, Xiong Y, Yue J, Xu D, Ihira K, Konno Y, Kobayashi N, Todo Y, Watari H. Long noncoding RNA NEAT1 drives aggressive endometrial cancer progression via miR-361-regulated networks involving STAT3 and tumor microenvironment-related genes. *J Exp Clin Cancer Res* 2019;**38**:295.

[18] Teng F, Tian WY, Wang YM, Zhang YF, Guo F, Zhao J, Gao C, Xue FX. Cancer-associated fibroblasts promote the progression of endometrial cancer via the SDF-1/CXCR4 axis. *J Hematol Oncol* 2016;**9**:8.

[19] Hui L, Chen Y. Tumor microenvironment: sanctuary of the devil. *Cancer Lett* 2015;**368**:7–13.

[20] Hu JL, Wang W, Lan XL, Zeng ZC, Liang YS, Yan YR, Song FY, Wang FF, Zhu XH, Liao WJ, et al. CAFs secreted exosomes promote metastasis and chemotherapy resistance by enhancing cell stemness and epithelial-mesenchymal transition in colorectal cancer. *Mol Cancer* 2019;**18**:91.

[21] Richards KE, Zeleniak AE, Fishel ML, Wu J, Littlepage LE, Hill R. Cancer-associated fibroblast exosomes regulate survival and proliferation of pancreatic cancer cells. *Oncogene* 2017;**36**:1770–8.

[22] Zomer A, Maynard C, Verweij FJ, Kamermans A, Schafer R, Beerling E, Schiffelers RM, de Wit E, Berenguer J, Ellenbroek SIJ, et al. Vivo imaging reveals extracellular vesicle-mediated phenocopying of metastatic behavior. *Cell* 2015;**161**:1046–57.

[23] Bach DH, Hong JY, Park HJ, Lee SK. The role of exosomes and miRNAs in drug-resistance of cancer cells. *Int J Cancer* 2017;**141**:220–30.

[24] Luga V, Zhang L, Viloria-Petit AM, Ogunjimi AA, Inanlou MR, Chiu E, Buchanan M, Hosein AN, Basik M, Wrana JL. Exosomes mediate stromal mobilization of autocrine Wnt-PCP signaling in breast cancer cell migration. *Cell* 2012;**151**:1542–56.

[25] Wang X, Pei X, Guo G, Qian X, Dou D, Zhang Z, Xu X, Duan X. Exosome-mediated transfer of long noncoding RNA H19 induces doxorubicin resistance in breast cancer. *J Cell Physiol* 2020.

[26] Xue M, Chen W, Xiang A, Wang R, Chen H, Pan J, Pang H, An H, Wang X, Hou H, et al. Hypoxic exosomes facilitate bladder tumor growth and development through transferring long non-coding RNA-UCA1. *Mol Cancer* 2017;**16**:143.

[27] Sun Q, Hao Q, Prasanth KV. Nuclear long noncoding RNAs: key regulators of gene expression. *Trends Genet* 2018;**34**:142–57.

[28] Karatas S, Sal V, Kahramanoglu I, Demirkiran F, Bese T, Arvas M, Sofiyeva N, Guralp O, Uzun H. Ykl-40 and cancer antigen 72-4 as new and promising diagnostic and prognostic markers for endometrial cancer. *Turk J Obstet Gynecol* 2018;**15**:235–42.

[29] Kotowicz B, Fuksiewicz M, Jonska-Gmyrek J, Wagrodzki M, Kowalska M. Preoperative serum levels of YKL 40 and CA125 as a prognostic indicators in patients with endometrial cancer. *Eur J Obstet Gynecol Reprod Biol* 2017;**215**:141–7.

[30] Salmena L, Poliseno L, Tay Y, Kats L, Pandolfi PP. A ceRNA hypothesis: the Rosetta Stone of a hidden RNA language? *Cell* 2011;**146**:353–8.

[31] Luo Y, Chen JJ, Lv Q, Qin J, Huang YZ, Yu MH, Zhong M. Long non-coding RNA NEAT1 promotes colorectal cancer progression by competitively binding miR-34a with SIRT1 and enhancing the Wnt/beta-catenin signaling pathway. *Cancer Lett* 2019;**440-441**:11–22.

[32] Wang M, Mao C, Ouyang L, Liu Y, Lai W, Liu N, Shi Y, Chen L, Xiao D, Yu F, et al. Long noncoding RNA LINC00336 inhibits ferroptosis in lung cancer by functioning as a competing endogenous RNA. *Cell Death Differ* 2019;**26**:2329–43.